Proceedings of the Combustion Institute, Volume 28, 2000/pp. 447–454

RADIATION AND NITRIC OXIDE FORMATION IN TURBULENT NON-PREMIXED JET FLAMES

J. H. FRANK, R. S. BARLOW AND C. LUNDQUIST*

Combustion Research Facility
Sandia National Laboratories
Livermore, CA 94551, USA

Radiative heat transfer has a significant effect on nitric oxide (NO) formation in turbulent non-premixed flames. Consequently, predictive models of turbulent non-premixed flames must include an accurate radiation submodel. To investigate the importance of radiation submodels in modeling NO formation, multiscalar measurements of temperature and species were coupled with radiation measurements in a series of turbulent non-premixed jet flames. A range of fuel mixtures were considered including H_2, H_2/He, $CO/H_2/N_2$, $CH_4/H_2/N_2$, and partially premixed CH_4/air. This group of flames represents a range of complexity with regard to NO formation and is currently the subject of multiple modeling efforts. Measurements of radiant fraction, temperature, and NO mass fraction have been compared with previously obtained modeling results for the H_2, H_2/He, and CH_4/air flames. The results show that an emission-only radiation submodel is adequate for modeling the hydrogen flames but not the CH_4/air flames. In one CH_4/air flame, the emission-only computations overpredict the radiant heat loss by a factor of 2.5. A comparison of adiabatic and radiative computations shows that the inclusion of radiative losses can reduce the predicted peak NO levels by as much as 57%. An accurate radiation submodel for hydrocarbon flames must account for radiative absorption. Spectrally resolved radiation calculations show that absorption by CO_2 near 4.3 μm is primarily responsible for the increased optical density of the hydrocarbon flames. The series of turbulent jet flames considered here contains a range of CO_2 levels and provide a basis for developing a realistic radiation model that incorporates absorption by CO_2.

Introduction

The capability to accurately model emissions of nitric oxide (NO) from combustion devices is an important step in the process of reducing air pollution. Predictive modeling of NO formation in turbulent non-premixed flames remains a significant challenge because of the complexity of the NO formation process and the sensitivity of NO results to several different submodels. Attempts to understand scaling relations between the NO emission index and various global flame parameters have had limited success [1]. The production of NO depends on a variety of parameters including local temperature, O-atom concentration, local mixing rates, global flame residence time, radiative heat loss, and, in hydrocarbon flames, the fuel-rich chemistry of prompt NO formation and reburn. There are thus multiple submodels that need to be validated before NO production can be accurately computed by turbulent combustion models. In the present work, we contribute to the investigation of the role of the radiation submodel in computing NO formation.

Previous work has shown that radiation plays a significant role in NO formation in hydrogen jet flames despite the relatively low values of radiant fractions [2,3]. Radiation has also been shown to play an important role in NO production in hydrocarbon flames [1,4]. Radiant fractions in hydrocarbon flames can be substantially higher than those of hydrogen flames because of the efficient broadband radiation from soot. Actual radiant fractions depend on the sooting tendency of the hydrocarbon fuel, the residence times within the flame, and the degree to which radiation is reabsorbed within the flame.

In the present study, we investigate radiative emission and NO formation in a series of non-sooting turbulent jet flames, in which radiative transfer is dominated by gas-molecular radiation. The flames considered here are included in the data library of the International Workshop on Measurement and Computation of Turbulent Nonpremixed Flames (TNF) [5], which has been established to facilitate collaborative comparisons of measured and modeled results. Velocity data and detailed scalar data, including NO, are available for each flame. Fuel compositions include H_2, H_2/He, $CO/H_2/N_2$, $CH_4/H_2/N_2$, and partially premixed CH_4/air. The use of non-sooting flames eliminates the additional complexity

*Present address: Department of Mechanical Engineering, University of California at Berkeley, Berkeley, CA 94546, USA.

Report Documentation Page

Form Approved
OMB No. 0704-0188

1. REPORT DATE **04 AUG 2000**	2. REPORT TYPE **N/A**	3. DATES COVERED **-**

4. TITLE AND SUBTITLE **Radiation and Nitric Oxide Formation in Turbulent Non-Premixed Jet Flames**	5a. CONTRACT NUMBER 5b. GRANT NUMBER 5c. PROGRAM ELEMENT NUMBER
6. AUTHOR(S)	5d. PROJECT NUMBER 5e. TASK NUMBER 5f. WORK UNIT NUMBER
7. PERFORMING ORGANIZATION NAME(S) AND ADDRESS(ES) **Combustion Research Facility Sandia National Laboratories Livermore, CA 94551, USA**	8. PERFORMING ORGANIZATION REPORT NUMBER
9. SPONSORING/MONITORING AGENCY NAME(S) AND ADDRESS(ES)	10. SPONSOR/MONITOR’S ACRONYM(S) 11. SPONSOR/MONITOR’S REPORT NUMBER(S)

12. DISTRIBUTION/AVAILABILITY STATEMENT
Approved for public release, distribution unlimited

13. SUPPLEMENTARY NOTES
See also ADM001790, Proceedings of the Combustion Institute, Volume 28. Held in Edinburgh, Scotland on 30 July-4 August 2000.

14. ABSTRACT

15. SUBJECT TERMS

16. SECURITY CLASSIFICATION OF:			17. LIMITATION OF ABSTRACT	18. NUMBER OF PAGES	19a. NAME OF RESPONSIBLE PERSON
a. REPORT **unclassified**	b. ABSTRACT **unclassified**	c. THIS PAGE **unclassified**	**UU**	**8**	

Standard Form 298 (Rev. 8-98)
Prescribed by ANSI Std Z39-18

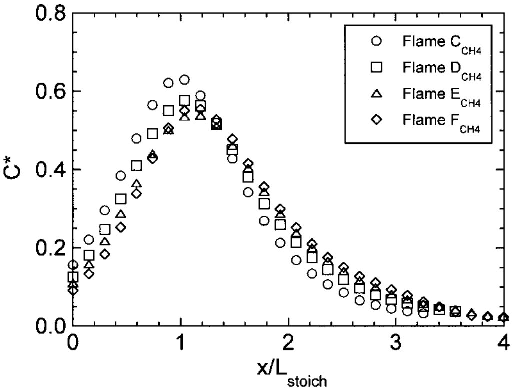

FIG. 1. Measured axial profiles of the normalized radiant power (C^*) from four partially premixed turbulent CH_4/air jet flames (3/1 air/fuel by vol.) with different Reynolds numbers. Flame conditions are given in Table 1. Values of C^* were determined using the total measured radiant power for normalization. The axial coordinate was normalized by the stoichiometric flame length.

of possible soot-NO interactions and reduces interference with the laser-based measurement techniques. Nevertheless, this series of fuels corresponds to an increasing scale of complexity with regard to NO formation. For example, the helium-diluted hydrogen flames have low levels of radiation, such that the influence of the radiation submodel on NO predictions is minimized, allowing a separate evaluation of submodels for coupling turbulence and chemistry [2]. The CO flames add the more strongly emitting and absorbing CO_2 molecule to the radiation problem, while retaining the relative simplicity of NO formation by the thermal mechanism alone. The non-sooting methane flames add complexity in a chemical kinetic sense, with the inclusion of prompt NO formation and reburn. The formation of NO is strongly affected by temperature in most of the jet flames considered by the TNF. Consequently, radiation submodels must be validated for a range of flames before the overall accuracy of NO predictions may be addressed.

In the following sections, we present measurements of radiant fractions for a series of TNF target flames. For several of the flames, computed radiant fractions were compared with the measurements. In one of the CH_4/air flames, measured spatial profiles of temperature and NO mass fraction were compared with both radiative and adiabatic model calculations. Radiation calculations using RADCAL [6] were then coupled with temperature and species measurements to study the validity of an optically thin assumption in the radiation submodel. The discussion focuses on the importance of accurate radiation submodels for modeling NO formation in turbulent jet flames.

Experimental Methods

Radiation Measurements

Radiation measurements were performed using a Schmidt-Boelter-type heat flux transducer (Medtherm 64P-1-22) with a 150° view angle. A zinc selenide (ZnSe) window was mounted on the face of the radiometer to minimize effects of convective cooling. This window had an approximately 70% optical transmission between 0.7 and 17 μm and passed the radiation emitted from the flame, while isolating the radiometer from air currents. The total radiant flux emitted by each flame was determined following the method of Sivathanu and Gore [7]. The radiometer was first oriented vertically and scanned along a radial trajectory in the nozzle exit plane out to a distance $r = L_{\mathrm{stoich}}/2$, where L_{stoich} is the stoichiometric flame length determined from the measured axial profile of the Favre-average mixture fraction. The radiometer was then turned to face horizontally toward the axis of the jet and scanned along the length of the flame. The radiant flux was then integrated over a cylindrical surface, which was closed at the base of the flame and open at the top to determine the total radiant power, $\dot{S}_{\mathrm{rad}}$, emitted from the flame.

Examples of the axial distributions of radiant power are shown in Fig. 1 for four partially premixed CH_4/air flames. In the figure, the radiant power is expressed in terms of a non-dimensional radiant power, C^*, defined as

$$C^*(x/L_{\mathrm{stoich}}) = \frac{4\pi R^2 \dot{s}_{\mathrm{rad}}(x/L_{\mathrm{stoich}})}{\dot{S}_{\mathrm{rad}}} \quad (1)$$

where R is the radial distance from the burner axis to the radiometer, and $\dot{s}_{\mathrm{rad}}$ is the radiated power as a function of axial position [7]. The C^* profiles for these four flames nearly collapse upon one another, with the peak heat release occurring between $x/L_{\mathrm{stoich}} = 1.0$ and 1.2. These measurements indicate that the error incurred by neglecting radiant loss through the top of the cylinder was small if the height of the axial traverse was 3 to 4 times the stoichiometric flame length.

The calibration of the Medtherm radiometer was verified using a copper calorimeter. This verification ensured that the factory calibration, which was performed with a uniform blackbody source, was valid for the spectral content and angular distribution of radiation from non-sooting jet flames. The calorimeter consisted of a copper disk (36.1 mm diameter × 3.2 mm thickness) with a known mass and a front surface coating of flat black paint having an absorptivity of 0.93 (±0.07). A type-K thermocouple was attached to the back side of the disk, and all but the front surface were foam insulated. Radiative and convective energy transfer rates were determined

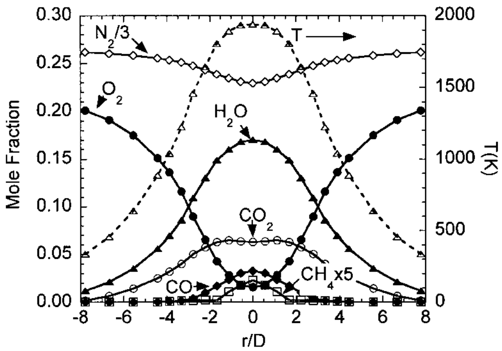

FIG. 2. Measurements of radial profiles of ensemble average temperature and species mole fractions in flame D_{CH_4} at $x/D = 45$. These profiles were used as input to the RADCAL calculations for investigating the optical density of the flame D_{CH_4}.

from measured heating and cooling curves. The convective transfer coefficient was calculated from the cooling curves and used to correct for convective energy loss during heating. Measurements of radiant flux were obtained using the two probes, and the results agreed within 5%, which was within the estimated uncertainty of $\pm 7\%$ for the calorimeter. All radiant fractions reported here were based on the original factory calibration of the radiometer.

Multiscalar Measurements

Experiments to obtain the multiscalar measurements included in the present paper were performed in the Turbulent Diffusion Flame (TDF) Laboratory at Sandia's Combustion Research Facility. Details of the flow facility and diagnostic apparatus have been described previously [8–11] and are not repeated here. Simultaneous point measurements of spontaneous Raman scattering, Rayleigh scattering, and laser-induced fluorescence (LIF) were used to determine temperature and the concentrations of CH_4, O_2, N_2, H_2O, CO_2, H_2, CO, OH, and NO. Fig. 2 displays multiscalar measurements of ensemble average temperature and major species for a radial profile in a turbulent partially premixed CH_4/air jet flame. Measured profiles such as these were used in our analysis of the optical density of selected flames. Estimated uncertainties (1σ) in averaged measurements of scalars used in the present analysis of radiation and in comparisons with model calculations were as follows: temperature 2–4%, CO_2 3–5%, H_2O 3–5%, and NO 10–20%. Further information on estimated uncertainties may be found in the references given above.

Results and Discussion

A series of turbulent axisymmetric jet flames with a range of fuel mixtures and flow conditions were considered. These flames are included in the TNF library, and detailed descriptions, including species, temperature, and velocity measurements, are available via the internet [5] and in the following references: H_2 and H_2/He flames [2,10,12]; CO/H_2/N_2 flames [11]; CH_4/H_2/N_2 flames [13]; partially premixed piloted CH_4/air flames [9,14,15]. Table 1 provides a brief overview of the flame conditions including fuel mixtures, jet Reynolds numbers, *Re*, stoichiometric flame length, L_{stoich}, and convective residence times, τ. The convective residence time was determined by $\tau = L_{stoich}/U_{jet}$, where U_{jet} is the jet exit velocity.

Radiation Results

Radiant fractions were measured for all the flames in Table 1. The radiant fraction, f_{rad}, is defined as

TABLE 1
Flame Conditions for Turbulent Jet Flames

Flame[a]	Fuel Mixture (by Volume)	*Re*	L_{stoich} (mm)	τ (ms)
A_{H_2}	100% H_2	10,000	476	1.6
B_{H_2}	80% H_2, 20% He	9,800	375	1.3
C_{H_2}	60% H_2, 40% He	8,300	270	1.1
A_{CHN}	40% CO, 30% H_2, 30% N_2	16,700	197	2.6
B_{CHN}	40% CO, 30% H_2, 30% N_2	16,700	340	7.5
A_{DLR}	22% CH_4, 33% H_2, 45% N_2	15,200	512	12.1
B_{DLR}	22% CH_4, 33% H_2, 45% N_2	22,800	544	8.6
C_{CH_4}	25% CH_4, 75% air	13,400	338	11.5
D_{CH_4}	25% CH_4, 75% air	22,400	338	6.9
E_{CH_4}	25% CH_4, 75% air	33,600	338	4.6
F_{CH_4}	25% CH_4, 75% air	44,800	338	3.4
F'_{CH_4}	25% CH_4, 75% air	42,600	338	3.6

[a]The present designation of flames is chosen to be consistent with those of the TNF Workshop [5].

TABLE 2
Experimental and Computational Radiant Fractions for Turbulent Jet Flames

Flame	f_{rad}[a] Exp	f_{rad} PDF	f_{rad} CMC
A_{H_2}	9.5%	12.3%	11.7%
B_{H_2}	~5.9%	7.3%	6.9%
C_{H_2}	~3.1%	3.0%	3.0%
A_{CHN}	3.4%		
B_{CHN}	7.1%		
A_{DLR}	9.1%		
B_{DLR}	7.4%		
C_{CH_4}	6.4%		
D_{CH_4}	5.1%	10.5%	12.5%
E_{CH_4}	4.1%		
F_{CH_4}	3.0%		
F'_{CH_4}	3.4%		

[a]In flames B_{H_2} and C_{H_2}, the radiometer used to measure f_{rad} had a sapphire window, which blocked radiation from the 6.3 μm water band. The values have been scaled based on measurements in flame A_{H_2} with the ZnSe window [2].

the ratio of the total radiated power, $\dot{S}_{rad}$, to the power released in the combustion reaction and is given by

$$f_{rad} \equiv \frac{\dot{S}_{rad}}{\dot{m}_{fuel}\Delta H_{comb}} \tag{2}$$

where $\dot{m}_{fuel}$ is the mass flow rate of the fuel, and ΔH_{comb} is the heat of combustion. The measured radiant fractions are listed in Table 2 for all the different turbulent jet flames.

For the flames considered here, radiation represents a relatively small portion of the total heat release, and the measured radiant fractions were less than 10%. The pure hydrogen flame, flame A_{H_2}, had one of the largest radiant fractions: 9.5%. However, the addition of helium dilution reduced the radiant fraction to 5.9% and 3.1% for 20% and 40% dilution, respectively. The helium dilution decreased the flame length and, thus, the residence time, which resulted in a lower radiant fraction. The reduced significance of radiation in the diluted hydrogen flames has previously been exploited to examine models of turbulence-chemistry coupling without the additional complexity of radiation effects [2]. That work includes an investigation of radiation and NO formation in flames A_{H_2}–C_{H_2}. A further analysis of the radiative properties of these three flames is reported here.

In the $CO/H_2/N_2$ flames, the radiant fraction increased from 3.4% to 7.1% when the nozzle diameter was increased by 68% and the Reynolds number was kept constant. This is a result of the increase in flame volume and residence time. For the $CH_4/H_2/N_2$ flames, the radiant fraction decreased from 9.1% to 7.4% when the Reynolds number was increased by 50%.

In the partially premixed CH_4/air flames, the values of f_{rad} ranged from 6.4% for flame C_{CH_4} to 3.0% in flame F_{CH_4}. The decrease in radiant fraction is primarily a result of the reduction in residence time. Flame F_{CH_4} exhibited a significant amount of localized extinction, and the radiant fraction was sensitive to the amount of extinction. As a measure of this sensitivity, we considered flame F'_{CH_4}, in which the flow velocity was reduced by 5% relative to that of flame F_{CH_4}. This slight reduction in flow velocity decreased the degree of extinction and resulted in a 13% relative increase in f_{rad} from flame F_{CH_4} to flame F'_{CH_4}. The sensitivity of f_{rad} to the initial flow conditions presents an additional challenge when comparing computations and measurements of flames with significant extinction.

Computed Radiant Fractions

Calculations and measurements of radiant fraction were compared for the pure H_2 and helium-diluted H_2 flames and for flame D_{CH_4} of the CH_4/air flame series. Values of f_{rad} were computed using both probability density function (PDF) and conditional moment closure (CMC) models of turbulent jet diffusion flames [2,16,17]. The calculated radiant fractions are included in Table 2. The combustion models were implemented using an optically thin assumption in the radiative submodel. This approach assumes that the absorption of radiation within the flame is insignificant and that each radiating point has an unimpeded view of the cold surroundings. The flame is assumed to be free of particles, including soot, and the only sources of radiant emission are gas-phase H_2O, CO_2, CO, and CH_4.

Radiative transfer in the H_2 flames essentially involves only H_2O. Relatively good agreement between calculated and measured radiant fractions was observed for flames A_{H_2}–C_{H_2}. The agreement improved with increased helium dilution. At 40% helium dilution, both the PDF and CMC calculations of f_{rad} agreed with the measurement. This suggests that the optically thin approximation is quite accurate for the diluted hydrogen flames and somewhat less accurate for the pure hydrogen flame. A more detailed analysis of the optical density of flame A_{H_2} is discussed later.

Calculating the radiant fraction in CH_4/air flames presents an additional challenge because both H_2O and CO_2 are major contributors to the radiative transfer. In flame D_{CH_4}, the PDF and CMC calculations overpredict f_{rad} by a factor of 2.1 and 2.5, respectively. Note that the PDF and CMC calculations were performed to maximum downstream locations of $x/D = 90$ and $x/D = 100$, respectively.

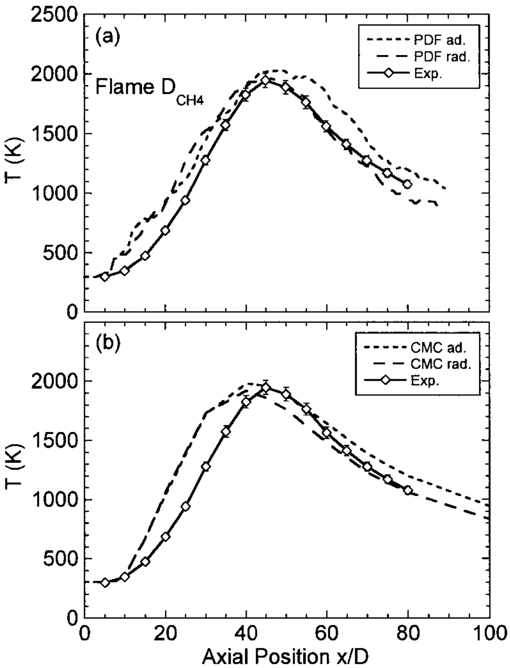

FIG. 3. Comparison of measured and computed centerline profiles of temperature in flame D_{CH_4}. Ensemble average experimental measurements (Exp.) are plotted with (a) PDF modeling results using adiabatic (PDF ad.) and radiative (PDF rad.) calculations and (b) CMC modeling results using adiabatic (CMC ad.) and radiative (CMC rad.) calculations. An emission-only radiation submodel was used in both the PDF and CMC radiative calculations.

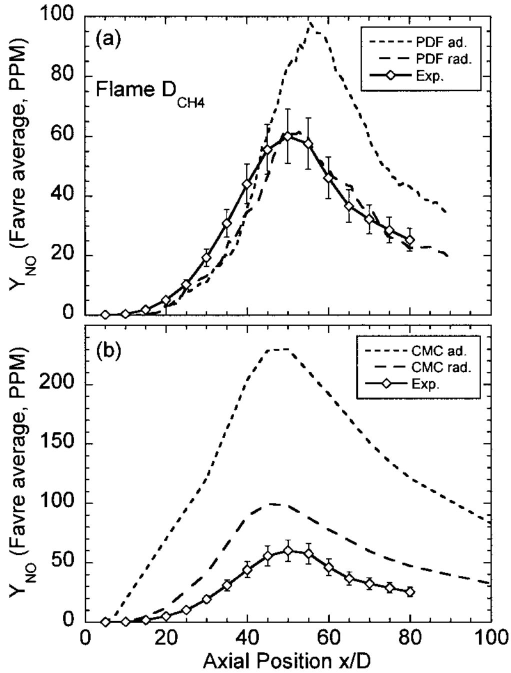

FIG. 4. Comparison of measured and computed centerline profiles of Favre-average NO mass fraction, Y_{NO}, in flame D_{CH_4}. Ensemble average experimental measurements (Exp.) are plotted with (a) PDF modeling results using adiabatic (PDF ad.) and radiative (PDF rad.) calculations and (b) CMC modeling results using adiabatic (CMC ad.) and radiative (CMC rad.) calculations. An emission-only radiation submodel is used in both the PDF and CMC radiative calculations.

When the extra 10-diameter difference is considered, the radiant fraction of the PDF calculation is actually somewhat closer to the 12.5% value, which was obtained for the CMC calculation. The large discrepancy between the calculations and the measurements of f_{rad} indicate that absorption by CO_2 is important in the CH_4/air jet flames.

A Comparative Example

The incorrect treatment of radiation in turbulent flame models can have a dramatic effect on the predicted NO levels. As an example of this effect, we considered modeling results with and without radiation for flame D_{CH_4}. Since the production of NO is highly dependent on temperature, we first compared temperature profiles. In Fig. 3, centerline temperature profiles from adiabatic and radiative computations for both the PDF (Fig. 3a) and the CMC (Fig. 3b) models are displayed along with ensemble average measurements. An optically thin assumption was used in the radiative calculations. The error bars for the measurements correspond to the uncertainties given above. For $x/D < \sim 40$, there is significant overlap of the adiabatic and radiative calculations, and both PDF and CMC calculations overpredict the temperature. This discrepancy is mainly due to differences in mixing, since radiation is not an important effect for this portion of the centerline profile. For $x/D > \sim 40$, the radiative calculations predict lower temperatures than do the adiabatic calculations, indicating the importance of radiative heat loss in this region. The average difference between the adiabatic and radiative calculations in the upper region of the flame is ~190 K and ~130 K for the PDF and CMC predictions, respectively.

The difference in the predicted temperature for the radiative and adiabatic calculations has a significant effect on the predicted NO levels. Fig. 4 shows a comparison of adiabatic and radiative calculations for centerline profiles of the Favre-average NO mass fraction, Y_{NO}. In Fig. 4a, the radiative PDF calculation shows a peak NO mass fraction that is 37% lower than the peak of the adiabatic calculation. The agreement of the radiative PDF calculation and the experiment is quite good. However, the optically

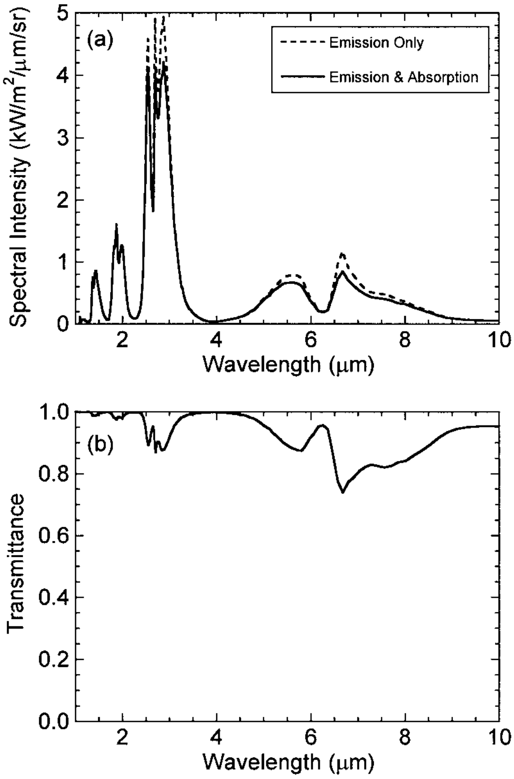

FIG. 5. Results of a line-of-sight radiation calculation for a radial cross section of the undiluted hydrogen jet flame, flame A_{H_2}, at a downstream location of $x/D = 34$. (a) Spectral intensity for emission-only and emission/absorption calculations. (b) Transmittance for the emission/absorption calculation.

thin radiation submodel does not accurately predict the radiant fraction in this flame. At this stage of the model development, the agreement between the calculated and measured NO profiles is considered fortuitous and suggests compensating errors. The peak value of Y_{NO} for the radiative CMC calculation (Fig. 4b) is 57% lower than the peak of the adiabatic calculation. A comparison of the CMC and PDF results in Figs. 3 and 4 reveals that the discrepancy between the adiabatic and radiative predictions of Y_{NO} does not scale with the differences in the temperature profiles. This reflects the complexity of the NO formation process and emphasizes the need to independently validate each submodel.

Optical Density of Flames

The above results show the importance of treating radiative transport carefully and suggest that both emission and absorption need to be considered in hydrocarbon flames. In order to better quantify the optical density of these flames, the RADCAL code was used to perform line-of-sight radiation calculations for selected radial measured profiles of temperature and species concentrations. The RADCAL code computes the total radiated power as well as the spectrally resolved radiant intensity and transmittance. Radial profiles of ensemble average species concentrations and temperature at a downstream location of $x/D = \sim L_{stoich}$ were used. This location corresponded to the peak radiative emission. Three representative flames from the above series of flames were considered: flames A_{H_2}, D_{CH_4}, and B_{CHN}. For each flame, two separate RADCAL calculations were performed, a normal emission/absorption calculation and an emission-only calculation.

The radiation calculation for flame A_{H_2} was used to investigate the validity of the optically thin assumption in hydrogen flames. This flame has the largest optical density of flames A_{H_2}–C_{H_2}. Fig. 5a shows the calculated spectral intensity of radiation from H_2O at a downstream location of $x/D = 34$. The difference between the optically thin and optically thick calculations is relatively small. The calculated value of total radiated power for the emission-only calculation is only 13% higher than that of the emission/absorption case. Fig. 5b shows that the small amount of absorption by H_2O resulted in a minimum transmittance of 74% at 6.7 μm. These results indicate that the optically thin assumption is adequate for the hydrogen flames.

The measured species and temperature profiles used in the RADCAL calculation for flame D_{CH_4} are shown in Fig. 2. The calculated value of total radiated power for the emission-only case is 39% higher than that of the emission/absorption computation. This indicates that optical absorption is important in flame D_{CH_4}. The calculated spectral distributions of the emission intensity and transmittance for flame D_{CH_4} are plotted in Fig. 6. Results for the 4.3 μm band of CO_2 show a significant effect of absorption over the measured flame profile. Fig. 6b shows that the transmittance for the emission/absorption calculation drops to a minimum of 17%. These results indicate that significant errors in the calculated radiant fraction should be expected if an optically thin, or emission-only, assumption is used in treating CO_2 radiation from these CH_4/air flames.

The CO/H_2 flames generate CO_2 levels approximately twice those in the CH_4/air flame. Consequently, absorption by CO_2 is expected to be even more significant. A radiation calculation was performed for flame B_{CHN}, which is the larger of the two CO/H_2 flames. The results of the RADCAL calculation are shown in Fig. 7. As was the case with flame D_{CH_4}, the most prominent feature is the CO_2 band near 4.3 μm. The peak spectral intensity in the emission/absorption calculation is only 13% higher than that for flame D_{CH_4} (see Fig. 6a). For the

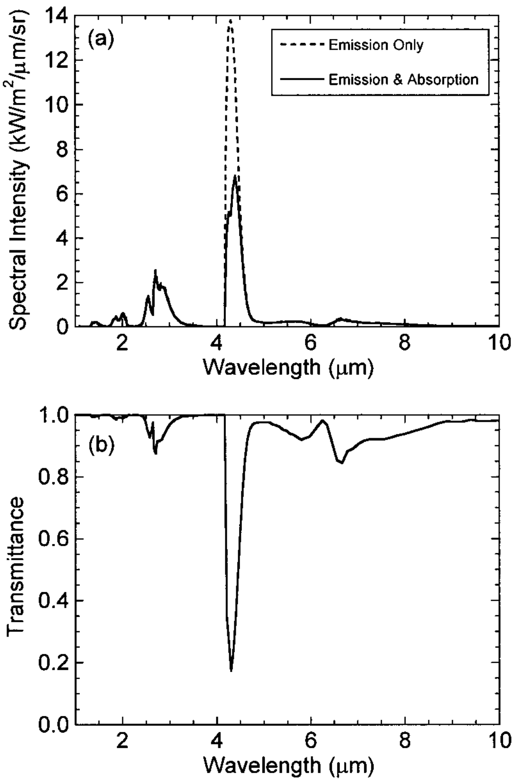

FIG. 6. Results of a line-of-sight radiation calculation for a radial cross section of flame D_{CH_4} at a downstream location of $x/D = 45$. The computation was performed using the measured radial profiles of species and temperature shown in Fig. 2. (a) Spectral intensity for emission-only and emission/absorption calculations. (b) Transmittance for the emission/absorption calculation.

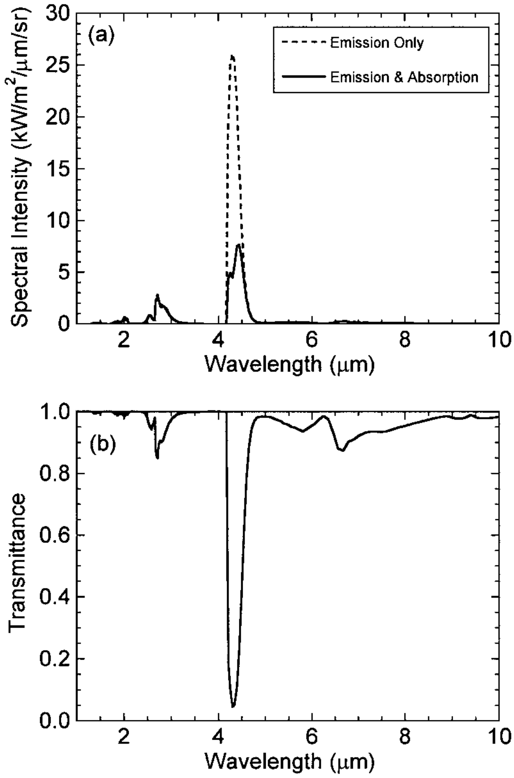

FIG. 7. Results of a line-of-sight radiation calculation for a radial cross section of flame B_{CHN} of the $CO/H_2/N_2$ flames at a downstream location of $x/D = 50$. (a) Spectral intensity for emission-only and emission/absorption calculations. (b) Transmittance for the emission/absorption calculation.

CO/H_2 flame, however, the difference between the emission-only and emission/absorption calculations is much more significant. The total emitted intensity for the emission-only calculation is 2.2 times that of the emission/absorption case. Fig. 7b shows that the transmittance associated with 4.3 μm band of CO_2 has a minimum of 4.5%. Clearly, the computation of NO formation in the $CO/H_2/N_2$ flames must include the radiative absorption of CO_2.

Conclusions

The importance of radiation in modeling NO formation was investigated for a series of turbulent nonpremixed jet flames using combined multiscalar diagnostics and radiometric measurements. Measurements of radiant fraction, temperature, and NO mass fraction were presented and compared with previous modeling results. The models included an emission-only radiation submodel, which we found to be adequate for pure hydrogen flames and helium-diluted hydrogen flames. However, in hydrocarbon flames, the optically thin assumption was inappropriate. In a partially premixed CH_4/air flame, computations overpredict the radiant fraction by a factor of 2.5. A comparison of results from radiative and adiabatic computations in this same flame demonstrated the sensitivity of the predicted NO levels to radiation. The inclusion of radiative losses with a radiant fraction of 12.5% resulted in a 57% reduction in predicted NO levels.

Further analysis of the spectral characteristics of the radiant emission and transmittance confirmed that an optically thin assumption is inappropriate for both the CO/H_2 and partially premixed CH_4/air jet flames. The primary source of radiative absorption was CO_2 in the 4.3 μm band. The need to incorporate optical absorption into radiation submodels complicates modeling efforts. A full radiative transfer calculation is computationally expensive, and an alternative method of including CO_2 absorption is needed for hydrocarbon jet flames. Previous efforts to incorporate radiation into modeling of turbulent nonpremixed flames include work with strongly radiating acetylene/air flames by Gore et al. [18]. The measurements and analysis presented here will serve as a basis for developing a valid radiation submodel for the TNF library of flames. Once the radiation submodel has been appropriately addressed, it will be feasible to study the effects of various aspects of the turbulence-chemistry models on NO formation. Since NO formation is less complex in CO/H_2 flames than in CH_4/air flames, it may be useful to first address the submodels for CO/H_2 flames.

Acknowledgments

This research was supported by the U.S. Department of Energy, Office of Basic Energy Sciences, Division of Chemical Sciences. The authors thank J. Gore and Y. Sivathanu for valuable discussions and contributions to initial radiation measurements. The authors thank J.-Y. Chen, R. Bilger, and M. Roomina for their contribution of modeling results.

REFERENCES

1. Turns, S. R., *Prog. Energy Combust. Sci.* 21:361–385 (1995).
2. Barlow, R. S., Smith, N. S. A., Chen, J.-Y., and Bilger, R. W., *Combust. Flame* 117:4–31 (1999).
3. Smith, N. S. A., Bilger, R. W., Carter, C. D., Barlow, R. S., and Chen, J.-Y., *Combust. Sci. Technol.* 105:357–375 (1995).
4. Turns, S. R., and Myhr, F. H., *Combust. Flame* 87:319–335 (1991).
5. Sandia National Laboratories, www.ca.sandia.gov/tdf/Workshop.html.
6. Grosshandler, W. L., *RADCAL: A Narrow-Band Model for Radiation Calculations in a Combustion Environment,* NIST technical note 1402, 1993.
7. Sivathanu, Y. R., and Gore, J. P., *Combust. Flame* 94:265–270 (1993).
8. Frank, J. H., and Barlow, R. S., *Proc. Combust. Inst.* 27:759–766 (1998).
9. Barlow, R. S., and Frank, J. H., *Proc. Combust. Inst.* 27:1087–1095 (1998).
10. Barlow, R. S., and Carter, C. D., *Combust. Flame* 97:261–280 (1994).
11. Barlow, R. S., Fiechtner, G. J., Carter, C. D., and Chen, J.-Y., *Combust. Flame* 120:549–569 (2000).
12. Barlow, R. S., and Carter, C. D., *Combust. Flame* 104:288–299 (1996).
13. Bergmann, V., Meier, W., Wolff, W., and Stricker, W., *Appl. Phys. B* 66:489–502 (1998).
14. Masri, A. R., Dibble, R. W., and Barlow, R. S., *Prog. Energy Combust. Sci.* 22:307–362 (1996).
15. Stårner, S. H., Bliger, R. W., and Barlow, R. S., *Combust. Sci. Technol.* 70:111–133 (1990); *Combust. Sci. Technol.* 72:255–269 (1990).
16. Chen, J.-Y., personal communication, 1999.
17. Roomina, M. R., and Bilger, R. W., *Combust. Flame*, in press (2001).
18. Gore, J. P., Ip, U.-S., and Sivathanu, Y. R., *ASME J. Heat Transfer* 114:487–493 (1992).

COMMENTS

Stephen B. Pope, Cornell University, USA. The absorption has been estimated based on mean profiles, that is, with the neglect of turbulent fluctuations. Can you quantify the impact of turbulent fluctuations on your conclusions.

Author's Reply. The use of ensemble average radial profiles of temperature and species concentrations in the RADCAL calculations did not account for the turbulence/radiation interactions. The quantitative evaluation of turbulence/radiation interactions requires measurements of the instantaneous radial profiles of temperature and species concentrations. The capability to perform such measurements is currently under development [1].

Previous results comparing predictions of mean and stochastic properties in both hydrogen/air and methane/air diffusion flames indicate that the turbulence/radiation interactions are important to consider but do not alter the conclusions of our analysis of the optical density of turbulent jet flames [2,3].

REFERENCES

1. Barlow, R. S., and Miles, P. C., *Proc. Combust. Inst.* 28:269–277 (2000).
2. Gore, J. P., Jeng, S.-M., and Faeth, G. M., *J. Heat Transfer* 109:165–171 (1987).
3. Jeng, S.-M., Lai, M.-C., and Faeth, G. M., *Combust. Sci. Technol.* 40:41–53 (1984).